Research Square

Preprints are preliminary reports that have not undergone peer review.
They should not be considered conclusive, used to inform clinical practice,
or referenced by the media as validated information.

Modeling and Analysis of Torsional Waves in Exponentially Graded Heterogeneous Multilayered Media with an Initially Stressed Poroelastic Layer

Dinesh Kumar Majhi
Patna University
Anurag Rakesh
anuragrakesh361@gmail.com
Patna University
Sumit Kumar Vishwakarma
Birla Institute of Technology and Science - Hyderabad Campus
Sunny Kumar
Patna University

Research Article

Keywords: Torsional surface waves, multilayered medium, exponential heterogeneity, poroelasticity, initial stress, dispersion relation

Posted Date: May 21st, 2026

DOI: https://doi.org/10.21203/rs.3.rs-8580557/v1

License: This work is licensed under a Creative Commons Attribution 4.0 International License.
Read Full License

Additional Declarations: No competing interests reported.

Modeling and Analysis of Torsional Waves in Exponentially Graded Heterogeneous Multilayered Media with an Initially Stressed Poroelastic Layer

Dinesh Kumar Majhi[1], Anurag Rakesh[2, *], Sumit Kumar Vishwakarma[3], Sunny Kumar[4]

[1]Department of Mathematics, Patna College, Patna University, Patna - 800005, India.

[2, 4]Department of Mathematics, Patna University, Patna - 800005, India.

[3]Department of Mathematics, BITS Pilani, Hyderabad Campus, Hyderabad - 500078, India.

[1]Email: dinesh.majhi@yahoo.com, [2, *]Email: anuragrakesh361@gmail.com,

[3]Email: sumitkumar@hyderabad.bits-pilani.ac.in, [4]Email: kumarsunnysharma96@gmail.com

ABSTRACT: The paper discusses torsional waves propagation through a multilayered medium consisting of exponentially varying heterogeneous transversely isotropic elastic upper layer and lower half-space; and an anisotropic poroelastic middle layer with initial stress. The governing equations for each region are derived using appropriate stress–strain relations and solved in terms of Whittaker functions and Bessel functions. By applying boundary and continuity conditions across the interfaces, a general dispersion relation is obtained, which incorporates the combined effects of material heterogeneity, poroelasticity, and pre-stress. Numerical analysis is undertaken to investigate the effect of key parameters, including rigidity and density inhomogeneity present in both upper layer and lower half-space, as well as initial compressive stress in the porous middle layer. The results show that rigidity heterogeneity has the most considerable effect on phase velocity, followed by density variation and initial stress effects. Specifically, increasing rigidity or compressive stress leads to a substantial rise in torsional wave velocity, while density variation contributes moderately to wave speed enhancement. The findings provide deeper insight into the role of heterogeneity and pre-stress in controlling characteristics of torsional wave, with potential applications in seismic exploration, subsurface imaging, and geotechnical engineering.

KEYWORDS: Torsional surface waves, multilayered medium, exponential heterogeneity, poroelasticity, initial stress, dispersion relation

1. INTRODUCTION

Earthquakes are complex geological events that involve tectonic plates movement and dissipation of energy in the crust of the Earth. Earthquakes occur due to the sudden movement along faults in

the Earth’s crust, which is often triggered by the release of built-up stress in underground rocks The seismic waves generated by this sudden movement cause the Earth to shake. Volcanic eruptions, snow avalanches, landslides and even turbulent rivers can also generate seismic waves which also can be detected and studied by seismologists. The Earth's interior is indeed complex and difficult to study through direct excavation. Advanced technologies for seismic wave propagation are the most credible and cost-effective methods for exploring the Earth's internal structure. For the purpose of understanding Earth's interior composition, various geophysical models have been developed by researchers that account for various material properties, including inhomogeneity, anisotropy, reinforcement, viscoelasticity and magneto elasticity, etc. In dynamic problems, these properties significantly influence seismic wave propagation and provide insights into the Earth's composition. The basic theory and core literature on elastic waves have been extensively covered in numerous books, scholarly works and monographs.

Beyond the extensive literatures on Love waves, Rayleigh waves, Stonely waves, we have another category of surface wave, known as torsional waves, which has garnered relatively limited attention. The study of this wave has got significant attention due to its broad implications in geophysics, civil engineering, and earthquake seismology. Among various wave types, torsional waves are uniquely sensitive to variations in shear properties, making them valuable for probing the mechanical behaviour of layered media. The foundational principles governing elastic behaviour in solid media were laid down in the classical works of Love [1] and Ewing et al. [4], which provided early insights into wave mechanics in layered structures. The complexity of wave propagation in realistic geological formations necessitates an understanding of layered, inhomogeneous, porous, and pre-stressed media, which has evolved over decades through both theoretical and experimental contributions. Biot’s pioneering work on propagation of wave for fluid-saturated porous solids [5], [6], as well as his exploration of incremental deformation mechanics [7], revolutionized the modelling of poroelastic media. His earlier study on wave behaviour under initial stress [2] highlighted critical role of pre-stress in modifying wave characteristics. These ideas were further extended by Weiskopf [3], who analysed stress distributions in soils, emphasizing the interaction between foundations and subsurface stress waves. Achenbach [9] and Bath [8] provided in-depth mathematical frameworks for wave propagation in elastic and seismological contexts, respectively, while Udías and Buforn [20] presented a modern consolidation of seismological principles applicable to surface waves.

Vardoulakis [10] contributed by analysing torsional wave behaviour in inhomogeneous elastic media, marking a key development in addressing geometric and material irregularities. Subsequent studies expanded these concepts to more complex environments. For instance, Dey and Sarkar [11] explored the behaviour of torsional waves in anisotropic and porous media subjected to initial stress, and later by Dey et al. [12] in porous elastic layered systems. The role of rigid boundaries and heterogeneous substrata was explored by Gupta et al. [13], [14], highlighting sensitivity of torsional surface wave behaviour to interface conditions and material gradation. Kumari and Sharma [15], [16] introduced viscoelastic and magneto-viscoelastic effects into the analysis, offering insights into layered composite responses. Recent investigations have incorporated gravitational effects, dry sandy geomedia, and sliding contact interfaces [17], [18], [19], [24], [27], along with increasingly realistic heterogeneous modelling. Studies such as those by Alam et al. [22] and Prasad and Kundu [23] further integrated poroelasticity with anisotropic and stress-induced heterogeneities. The impact of corrugated boundaries, void-type porous materials, and numerical modelling has also been investigated in modern works [25], [28], [29]. The most recent contributions continue to refine these models. Shokrollahi et al. [26] presented a unified approach for both elastic and poroelastic layers, while Majhi et al. [30] offered insights into the combined effects of non-homogeneity and initial stress in layered poroelastic configurations. These cumulative efforts establish a robust platform for analysing torsional surface wave behaviour in complex geological structures.

This work examines the propagation attributes of torsional surface waves through a multilayered system, comprising upper layer and lower half-space with exponentially varying rigidity and density, sandwiching an initially stressed poroelastic middle layer. Such a configuration is of practical relevance in modelling the Earth's crust, where mechanical properties often vary continuously with depth due to compaction, weathering, and other geological processes. Exponential variation in rigidity and density is a realistic representation of these gradual changes, capturing the nonlinear behaviour of real-world media more effectively than uniform or linearly varying models. The middle layer, considered poroelastic and subject to initial stress, reflects conditions found in fluid-saturated geological formations, such as aquifers and hydrocarbon reservoirs, where pre-stress and porosity significantly influence wave propagation. The initial stress in poroelastic middle layer adds complexity to the wave propagation dynamics, modifying dispersion behaviour and potentially altering phase velocities. This research aims to develop a

comprehensive analytical framework to describe the wave propagation under these conditions. The equations that govern the dynamics of each layer are formulated and solved using appropriate boundary and continuity conditions, leading to a dispersion equation that encapsulates the effects of material gradation, poroelasticity, and initial stress. The results provide insights into how these factors collectively influence torsional wave characteristics, offering valuable implications for geotechnical assessment and subsurface imaging.

The findings provide critical data for improving the accuracy of seismic surveys used to locate natural resources by better predicting wave propagation through heterogeneous layers. The developed dispersion relations can enhance imaging techniques used to map the Earth's interior, particularly in identifying the properties of fluid-saturated zones like hydrocarbon reservoirs. The study's insights into material gradation and pre-stress are valuable for assessing the stability of soil and rock formations for large-scale construction projects and foundation designs. Understanding the role of initial stress and material heterogeneity helps in more accurately modeling seismic energy dissipation and ground shaking during tectonic events. Numerical results showing rigidity's dominant influence guide tomographic techniques to resolve depth-dependent stiffness changes in poroelastic media. Phase velocity variations due to heterogeneity and initial stress parameters inform inversion models for imaging underground formations, such as aquifers or fault zones.

2. FORMULATION

This investigation explores torsional waves propagation in a stratified medium composed of three distinct layers. The topmost heterogeneous layer having finite thickness H_2, characterized by rigidity and density varying exponentially. Beneath this lies a finite porous layer of thickness H_1, modelled as a water-saturated, anisotropic medium of Weiskopf type. The lowest region is an infinitely extending heterogeneous half-space, also exhibiting exponential gradation in rigidity as well as density. Intermediate porous layer under the influence of an initial compressive radial stress $P = -s_{rr}$, which introduces pre-stress effects into the wave dynamics. Anisotropy in the porous medium is incorporated to more accurately reflect directional dependence of mechanical properties

in naturally occurring formations. The configuration and boundary interfaces are illustrated schematically in Fig. 1.

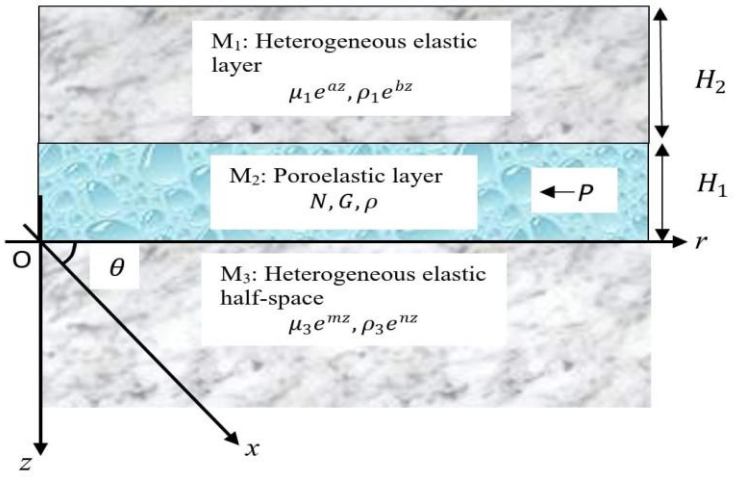


Fig. 1 Geometry of the problem

3. SOLUTIONS

3.1. DISPLACEMENT FOR M_1

We have motion equation governing the dynamics of the layer as

$$\frac{\partial \sigma_{r\theta}}{\partial r} + \frac{\partial \sigma_{z\theta}}{\partial z} + \frac{2}{r}\sigma_{r\theta} = \rho(z)\frac{\partial^2 v}{\partial t^2} \tag{1}$$

Here, $\sigma_{r\theta}$ and $\sigma_{z\theta}$ represent shear stress components, $v(r, \theta, z)$ stands for displacement in circumferential θ-direction, ρ stands for density of medium.

The corresponding stress-strain relationships in cylindrical coordinates are expressed as

$$\sigma_{r\theta} = \mu(z)\left(\frac{\partial v}{\partial r} - \frac{v}{r}\right), \sigma_{z\theta} = \mu(z)\left(\frac{\partial v}{\partial z}\right) \tag{2}$$

Substituting these relations (2) into (1), we get

$$\mu(z)\left(\frac{\partial^2 v}{\partial r^2} + \frac{1}{r}\frac{\partial v}{\partial r} - \frac{v}{r^2}\right) + \frac{\partial}{\partial z}\left(\mu(z)\frac{\partial v}{\partial z}\right) = \rho(z)\frac{\partial^2 v}{\partial t^2} \tag{3}$$

Assuming a separable solution as

$$v = V(z)J_1(kr)e^{i\omega t} \tag{4}$$

where k stands for wave number, $J_1(kr)$ for the first-order first kind Bessel function, ω for the angular frequency, Eq. (3) simplifies to

$$V''(z) + \frac{\mu'(z)}{\mu(z)} V'(z) - k^2 \left(1 - \frac{c^2}{c_z^2}\right) V(z) = 0 \tag{5}$$

Here, $c = \frac{\omega}{k}$ denotes phase velocity, the shear wave speed is defined as $c_z = \sqrt{\frac{\mu}{\rho}}$

Now, we consider exponentially varying material properties given by

$$\mu = \mu_1 e^{az}, \rho = \rho_1 e^{bz} \tag{6}$$

Substituting Eq. (6) into Eq. (5) yields

$$V''(z) + aV'(z) - k^2 \left[1 - \frac{c^2 e^{bz}}{c_1^2 e^{az}}\right] V(z) = 0 \tag{7}$$

where $c_1 = \sqrt{\frac{\mu_1}{\rho_1}}$

To eliminate the first derivative term $\frac{dV}{dz}$, we substitute $V(z) = \varphi(z) e^{\left(\frac{-az}{2}\right)}$ into Eq. (7), and obtain

$$\varphi''(z) - \left[\frac{a^2}{4} + k^2 \left\{1 - \frac{c^2}{c_1^2} \frac{(1+bz)}{(1+az)}\right\}\right] \varphi(z) = 0 \tag{8}$$

Introducing dimensionless parameters $\gamma_1 = \left(1 + \frac{a^2}{4k^2} - \frac{bc^2}{ac_1^2}\right)^{\frac{1}{2}}$ and $\eta_1 = \frac{2\gamma_1 k}{a}(1 + az)$ and letting $\varphi(z) = \psi(\eta_1)$, Eq. (8) transforms into

$$\psi''(\eta_1) - \left[\frac{1}{4} - \frac{H}{\eta_1}\right] \psi(\eta_1) = 0 \tag{9}$$

where the constant H is defined by $H = \frac{c^2(a-b)k}{2c_1^2 a^2 \gamma_1}$

The Whittaker differential equation, Eq. (9), has a general solution of the form

$$\psi(\eta_1) = A_1 W_{H,\frac{1}{2}}(\eta_1) + B_1 W_{-H,\frac{1}{2}}(-\eta_1) \tag{10}$$

Here A_1 and B_1 represent arbitrary constants.

Therefore, displacement for M_1 becomes

$$v = V(z)J_1(kr)e^{i\omega t}$$

$$= \varphi(z)e^{\left(\frac{-az}{2}\right)}J_1(kr)e^{i\omega t}$$

$$= \left[A_1 W_{H,\frac{1}{2}}\left(\frac{2\gamma_1 k}{a}(1+az)\right) + B_1 W_{-H,\frac{1}{2}}\left(-\frac{2\gamma_1 k}{a}(1+az)\right)\right] e^{\left(\frac{-az}{2}\right)}J_1(kr)e^{i\omega t} \quad (11)$$

3.2. DISPLACEMENT FOR M_2

We have governing equations of poroelastic medium subjected to compressive initial stress, as derived by Biot and Weiskopf, are given below

$$\frac{\partial s_{rr}}{\partial r} + \frac{1}{r}\frac{\partial s_{r\theta}}{\partial \theta} + \frac{\partial s_{rz}}{\partial z} + \frac{s_{rr}-s_{\theta\theta}}{r} - P\left(\frac{\partial \omega_z}{\partial \theta} - \frac{\partial \omega_\theta}{\partial z}\right) = \frac{\partial^2}{\partial t^2}(\rho_{rr}u + \rho_{r\theta}U) \quad (12)$$

$$\frac{\partial s_{r\theta}}{\partial r} + \frac{1}{r}\frac{\partial s_{\theta\theta}}{\partial \theta} + \frac{\partial s_{\theta z}}{\partial z} + \frac{2}{r}s_{r\theta} - P\frac{\partial \omega_z}{\partial r} = \frac{\partial^2}{\partial t^2}(\rho_{rr}v + \rho_{r\theta}V) \quad (13)$$

$$\frac{\partial s_{rz}}{\partial r} + \frac{1}{r}\frac{\partial s_{\theta z}}{\partial \theta} + \frac{\partial s_{zz}}{\partial z} + \frac{1}{r}s_{rz} - P\frac{\partial \omega_\theta}{\partial r} = \frac{\partial^2}{\partial t^2}(\rho_{rr}w + \rho_{r\theta}W) \quad (14)$$

$$\frac{\partial s}{\partial r} = \frac{\partial^2}{\partial t^2}(\rho_{r\theta}u + \rho_{\theta\theta}U) \quad (15)$$

$$\frac{\partial s}{\partial \theta} = \frac{\partial^2}{\partial t^2}(\rho_{r\theta}v + \rho_{\theta\theta}V) \quad (16)$$

$$\frac{\partial s}{\partial z} = \frac{\partial^2}{\partial t^2}(\rho_{r\theta}w + \rho_{\theta\theta}W) \quad (17)$$

Here, s_{ij} represent the incremental stress components, (u, v, w) stand for solid and (U, V, W) for fluid components of displacement respectively, s denotes stress in fluid. For rotation vector ω, components are expressed as

$$\omega_r = \frac{1}{2r}\left[\frac{\partial w}{\partial \theta} - r\frac{\partial v}{\partial z}\right], \omega_\theta = \frac{1}{2}\left[\frac{\partial u}{\partial z} - \frac{\partial w}{\partial r}\right], \omega_z = \frac{1}{2r}\left[\frac{\partial (rv)}{\partial r} - \frac{\partial v}{\partial \theta}\right] \quad (18)$$

For a porous, anisotropic, fluid-saturated layer with initial stress P, following are relationships between stress and strain

$$s_{rr} = (A+P)e_{rr} + (A-2N+P)e_{\theta\theta} + (F+P)e_{zz} + Q\varepsilon$$

$$s_{\theta\theta} = (A-2N)e_{rr} + Ae_{\theta\theta} + Fe_{zz} + Q\varepsilon$$

$$s_{zz} = Fe_{rr} + Fe_{\theta\theta} + Ce_{zz} + Q\varepsilon$$

$$s_{r\theta} = 2Ne_{r\theta}, s_{\theta z} = 2Ge_{\theta z}, s_{rz} = 2Ge_{zr} \quad (19)$$

where A, F, C, N, G are elastic coefficients. N and G also denote directional rigidities of anisotropic layer in r and z-directions respectively.

The strain components are defined as

$$e_{rr} = \frac{\partial u}{\partial r}, e_{\theta\theta} = \frac{1}{r}\frac{\partial v}{\partial \theta} + \frac{u}{r}, e_{zz} = \frac{\partial w}{\partial z},$$
$$e_{r\theta} = \frac{1}{2}\left[\frac{1}{r}\frac{\partial u}{\partial \theta} + \frac{\partial v}{\partial r} - \frac{v}{r}\right], e_{\theta z} = \frac{1}{2}\left[\frac{\partial v}{\partial z} + \frac{1}{r}\frac{\partial w}{\partial \theta}\right], \quad (20)$$
$$e_{zr} = \frac{1}{2}\left[\frac{\partial w}{\partial r} + \frac{\partial u}{\partial z}\right], \varepsilon = \left[\frac{1}{r}\frac{\partial (rU)}{\partial r} + \frac{1}{r}\frac{\partial V}{\partial \theta} + \frac{\partial W}{\partial z}\right]$$

Q serves as coupling parameter between the volumetric strain of solid and fluid components, and is positive. The stress vector from fluid pressure P relates to the total stress s as

$$-s = fP \quad (21)$$

where f stands for porosity.

Now mass densities of solid ρ_s, fluid ρ_f, and porous medium ρ relate to the mass coefficients ρ_{rr}, $\rho_{r\theta}$, $\rho_{\theta\theta}$ by

$$\rho_{rr} + \rho_{r\theta} = (1-f)\rho_s, \ \rho_{r\theta} + \rho_{\theta\theta} = f\rho_f \quad (22)$$

Aggregate mass density is depicted by

$$\rho = \rho_s + f(\rho_f - \rho_s) \quad (23)$$

According to Biot, the following inequalities must hold for physical validity

$$\rho_{r\theta} < 0, \rho_{rr} > 0, \ \rho_{\theta\theta} > 0, \rho_{rr}\rho_{\theta\theta} - \rho_{r\theta}^2 > 0 \quad (24)$$

Assuming propagation of torsional wave along r-direction with displacement in θ-direction, we consider

$$u = 0, v = v(r, z, t), w = 0$$
$$U = 0, V = V(r, z, t), W = 0 \quad (25)$$

With these assumptions, only the following stress-strain relations remain valid

$$s_{\theta z} = 2Ge_{\theta z}, s_{r\theta} = 2Ne_{r\theta} \tag{26}$$

Substituting these into the equations of motion (12) - (17), the only non-zero equation becomes

$$\frac{\partial s_{r\theta}}{\partial r} + \frac{\partial s_{\theta z}}{\partial z} + \frac{2}{r}s_{r\theta} - P\frac{\partial \omega_z}{\partial r} = \frac{\partial^2}{\partial t^2}(\rho_{rr}v + \rho_{r\theta}V) \tag{27}$$

and $$\frac{\partial^2}{\partial t^2}(\rho_{r\theta}v + \rho_{\theta\theta}V) = 0 \tag{28}$$

Using the stress-strain relations of Eq. (19) in Eq. (27), we get

$$\left(N - \frac{P}{2}\right)\left(\frac{\partial^2 v}{\partial r^2} - \frac{v}{r^2} + \frac{1}{r}\frac{\partial v}{\partial r}\right) + G\frac{\partial^2 v}{\partial z^2} = \frac{\partial^2}{\partial t^2}(\rho_{rr}v + \rho_{r\theta}V) \tag{29}$$

Using Eq. (28), assume $\rho_{r\theta}v + \rho_{\theta\theta}V = d''$ (constant), then

$$V_2 = \frac{d'' - \rho_{r\theta}v}{\rho_{\theta\theta}}$$

So, $$\frac{\partial^2}{\partial t^2}(\rho_{r\theta}v + \rho_{\theta\theta}V) = d'\frac{\partial^2 v}{\partial t^2} \tag{30}$$

where $d' = \rho_{rr} - \frac{\rho_{r\theta}^2}{\rho_{\theta\theta}}$

Substituting this into Eq. (29), we get

$$\left(N - \frac{P}{2}\right)\left(\frac{\partial^2 v}{\partial r^2} - \frac{v}{r^2} + \frac{1}{r}\frac{\partial v}{\partial r}\right) + G\frac{\partial^2 v}{\partial z^2} = d'\frac{\partial^2 v}{\partial t^2} \tag{31}$$

From Eq. (31), $\left[\frac{N-\frac{P}{2}}{d'}\right]^{\frac{1}{2}}$ and $\left(\frac{G}{d'}\right)^{\frac{1}{2}}$ are wave speeds obtained in r and z-directions, respectively.

For porous media, velocity β' for shear wave in r-direction has been expressed as

$\beta' = \left[\frac{1-\zeta}{d}c_2^2\right]^{\frac{1}{2}}$, here $c_2 = \sqrt{\frac{N}{\rho}}$ depicts velocity of shear wave in r-direction for anisotropic, non-porous elastic medium, with no initial stress.

Here, $\zeta = \frac{P}{2N}$, $d = \frac{d'}{\rho} = \frac{1}{\rho}\left(\rho_{rr} - \frac{\rho_{r\theta}^2}{\rho_{\theta\theta}}\right) = \gamma_{11} - \frac{\gamma_{12}^2}{\gamma_{22}}$

where $\gamma_{11} = \frac{\rho_{rr}}{\rho}, \gamma_{12} = \frac{\rho_{r\theta}}{\rho}, \gamma_{22} = \frac{\rho_{\theta\theta}}{\rho}$ are non-dimensional mass parameters defined by Biot for porous layer.

Introducing non-dimensional coordinates $\xi = \xi_0 + \frac{z}{L}$ and $R = \frac{r}{L}$, with wave number $k = \frac{1}{L}$, Eq. (31) becomes

$$\frac{\partial^2 v}{\partial R^2} + \frac{1}{R}\frac{\partial v}{\partial R} - \frac{v}{R^2} + \frac{G}{N - \frac{P}{2}}\frac{\partial^2 v}{\partial \xi^2} = \frac{d' L^2}{N - \frac{P}{2}}\frac{\partial^2 v}{\partial t^2} \tag{32}$$

Assuming solution of Eq. (32) as $v = V(\xi) J_1(R) e^{i\omega t}$, where $J_1(R)$ stands for first kind Bessel function, $V(\xi)$ is the solution of following ODE

$$\frac{d^2 V}{d\xi^2} + q^2 V = 0 \tag{33}$$

where $q^2 = \frac{\left(\frac{\omega^2 L^2 d'}{N - \frac{P}{2}} - 1\right)}{\frac{G}{N - \frac{P}{2}}}$

Eq. (33) has general solution given by

$$V(\xi) = A_2 e^{iq\xi} + B_2 e^{-iq\xi}$$

Hence, displacement for M_2 is

$$v = \left(A_2 e^{iq\xi} + B_2 e^{-iq\xi}\right) J_1(R) e^{i\omega t} \tag{34}$$

where $q^2 = d\upsilon \left(\frac{c^2}{c_2^2} - \frac{1-\zeta}{d}\right), \upsilon = \frac{N}{G}$, $c = \omega L$ is the phase velocity.

3.3. DISPLACEMENT FOR M_3

We have equation describing torsional wave motion in lower half-space, which possesses spatially varying properties, is given by

$$\frac{\partial \sigma_{r\theta}}{\partial r} + \frac{\partial \sigma_{z\theta}}{\partial z} + \frac{2}{r}\sigma_{r\theta} = \rho(z)\frac{\partial^2 v}{\partial t^2} \tag{35}$$

Here, $\sigma_{r\theta}$ and $\sigma_{z\theta}$ are the stress components, $v(r, \theta, z)$ stands for θ-direction displacement, ρ denotes material density.

We have stress-strain relationships expressed as

$$\sigma_{r\theta} = \mu\left[\frac{\partial v}{\partial r} - \frac{v}{r}\right], \sigma_{z\theta} = \rho\frac{\partial v}{\partial z} \tag{36}$$

Substituting these into the motion Eq. (35) gives

$$\mu(z)\left(\frac{\partial^2 v}{\partial r^2} + \frac{1}{r}\frac{\partial v}{\partial r} - \frac{v}{r^2}\right) + \frac{\partial}{\partial z}\left\{\mu(z)\frac{\partial v}{\partial z}\right\} = \rho(z)\frac{\partial^2 v}{\partial t^2} \tag{37}$$

Assuming solution as

$$v = V(z)J_1(kr)e^{i\omega t} \tag{38}$$

we reduce the governing equation to

$$V''(z) + \frac{\mu'(z)}{\mu(z)}V'(z) - k^2\left(1 - \frac{c^2}{c_z^2}\right)V(z) = 0 \tag{39}$$

where $c = \frac{\omega}{k}$ and $c_z = \sqrt{\frac{\mu}{\rho}}$

Given, $\mu = \mu_3 e^{mz}$, $\rho = \rho_3 e^{nz}$ (40)

Substituting into the differential Eq. (39), we obtain

$$V''(z) + mV'(z) - k^2\left[1 - \frac{c^2 e^{nz}}{c_3^2 e^{mz}}\right]V(z) = 0 \tag{41}$$

where $c_3 = \sqrt{\frac{\mu_3}{\rho_3}}$

To eliminate the first derivative $\frac{dV}{dz}$, we define $V(z) = \varphi(z)e^{\left(\frac{-mz}{2}\right)}$ which transforms the Eq. (41) into

$$\varphi''(z) - \left[\frac{m^2}{4} + k^2\left\{1 - \frac{c^2}{c_3^2}\frac{(1+nz)}{(1+mz)}\right\}\right]\varphi(z) = 0 \tag{42}$$

Introducing dimensionless variables $\gamma_3 = \left(1 + \frac{m^2}{4k^2} - \frac{nc^2}{mc_3^2}\right)^{\frac{1}{2}}$, $\eta_3 = \frac{2\gamma_3 k}{m}(1 + mz)$ and setting $\varphi(z) = \psi(\eta_3)$, Eq. (42) becomes

$$\psi''(\eta_3) - \left[\frac{1}{4} - \frac{S}{\eta_3}\right]\psi(\eta_3) = 0 \tag{43}$$

where $S = \frac{c^2(m-n)k}{2c_3^2 m^2 \gamma_3}$

For physical feasibility, the displacement should vanish as $z \to \infty$, corresponding to $\psi(\eta_3) \to 0$ as $\eta_3 \to \infty$. The bounded solution satisfying this behavior is

$$\psi(\eta_3) = DW_{S,\frac{1}{2}}(\eta_3)$$

where $W_{S,\frac{1}{2}}(\eta_3)$ depicts Whittaker function, D represents arbitrary constant.

Hence, displacement for M_3 becomes

$$v = V(z)J_1(kr)e^{i\omega t}$$

$$= \varphi(z)e^{\left(\frac{-mz}{2}\right)}J_1(kr)e^{i\omega t}$$

$$= \left[DW_{S,\frac{1}{2}}\left(\frac{2\gamma_3 k}{m}(1+mz)\right)\right]e^{\left(\frac{-mz}{2}\right)}J_1(kr)e^{i\omega t} \quad (44)$$

4. BOUNDARY CONDITIONS

We have corresponding boundary conditions as given below.

(i) At the interface of M_2 and M_3, continuity of displacements and stresses is required, i.e., at $z = 0$

(a) $[v]_2 = [v]_3$

(b) $[s_{\theta z}]_2 = [\sigma_{\theta z}]_3$

(ii) At the interface of M_1 and M_2, continuity of displacements and stresses is required, i.e., at $z = -H_1$

(a) $[v]_1 = [v]_2$

(b) $[\sigma_{\theta z}]_1 = [s_{\theta z}]_2$

(iii) The free surface of M_1 has no traction, i.e., at $z = -(H_1 + H_2)$

$[\sigma_{\theta z}]_1 = 0$

5. DISPERSION RELATION

Boundary conditions (i), (ii), and (iii) lead to

$$A_2 e^{iq\xi_0} + B_2 e^{-iq\xi_0} - DK_1 = 0 \tag{45}$$

$$A_2 K_2 e^{iq\xi_0} - B_2 K_2 e^{-iq\xi_0} - DK_3 = 0 \tag{46}$$

$$A_1 K_4 + B_1 K_5 - A_2 e^{iq\left(\xi_0 - kH_1\right)} - B_2 e^{-iq\left(\xi_0 - kH_1\right)} = 0 \tag{47}$$

$$A_1 R_1 e^{-\frac{\gamma_1 k}{a} + K_9 H_1} + B_1 R_2 e^{\frac{\gamma_1 k}{a} - K_{14} H_1} - A_2 K_2 e^{iq\left(\xi_0 - kH_1\right)} + B_2 K_2 e^{-iq\left(\xi_0 - kH_1\right)} = 0 \tag{48}$$

$$A_1 R_3 e^{-\frac{\gamma_1 k}{a} + K_9 (H_1 + H_2)} + B_1 R_4 e^{\frac{\gamma_1 k}{a} - K_{14} (H_1 + H_2)} = 0 \tag{49}$$

where

$$K_1 = W_{S,\frac{1}{2}}\left(\frac{2\gamma_3 k}{m}\right),\ K_2 = iGkq,$$

$$K_3 = \mu_3 \left(\frac{2\gamma_3 k}{m}\right)^S e^{\frac{-\gamma_3 k}{m}} \left[\frac{-m^2}{2\gamma_3 k}\left\{\frac{1}{4} - \left(S - \frac{1}{2}\right)^2\right\} + \left(mS - \gamma_3 k - \frac{m}{2}\right)\left\{1 + \frac{m}{2\gamma_3 k}\left\{\frac{1}{4} - \left(S - \frac{1}{2}\right)^2\right\}\right\}\right],$$

$$K_4 = W_{H,\frac{1}{2}}\left(\frac{2\gamma_1 k}{a}(1 - aH_1)\right) e^{\frac{aH_1}{2}},\ K_5 = W_{-H,\frac{1}{2}}\left(-\frac{2\gamma_1 k}{a}(1 - aH_1)\right) e^{\frac{aH_1}{2}},$$

$$K_6 = \left(\frac{2\gamma_1 k}{a}\right)^H (1 - aH_1)^H,\ K_7 = \frac{a^2}{2\gamma_1 k}\frac{\left(H - \frac{1}{2}\right)^2 - \frac{1}{4}}{(1 - aH_1)^2},\ K_8 = 1 + \frac{\frac{1}{4} - \left(H - \frac{1}{2}\right)^2}{\frac{2\gamma_1 k}{a}(1 - aH_1)},$$

$$K_9 = \gamma_1 k + \frac{a}{2},\ K_{10} = \frac{aH}{1 - aH_1},\ K_{11} = \left(\frac{2\gamma_1 k}{a}\right)^{-H} (1 - aH_1)^{-H},\ K_{12} = \frac{a^2}{2\gamma_1 k}\frac{\left(-H - \frac{1}{2}\right)^2 - \frac{1}{4}}{(1 - aH_1)^2},$$

$$K_{13} = 1 - \frac{\frac{1}{4} - \left(-H - \frac{1}{2}\right)^2}{\frac{2\gamma_1 k}{a}(1 - aH_1)},\ K_{14} = \gamma_1 k - \frac{a}{2},\ K_{15} = \left(\frac{2\gamma_1 k}{a}\right)^H \left(1 - a(H_1 + H_2)\right)^H,$$

$$K_{16} = \frac{a^2}{2\gamma_1 k}\frac{\left(H - \frac{1}{2}\right)^2 - \frac{1}{4}}{\left(1 - a(H_1 + H_2)\right)^2},\ K_{17} = 1 + \frac{\frac{1}{4} - \left(H - \frac{1}{2}\right)^2}{\frac{2\gamma_1 k}{a}\left(1 - a(H_1 + H_2)\right)},\ K_{18} = \frac{aH}{1 - a(H_1 + H_2)},$$

$$K_{19} = \left(\frac{2\gamma_1 k}{a}\right)^{-H} \left(1 - a(H_1 + H_2)\right)^{-H},\ K_{20} = \frac{a^2}{2\gamma_1 k}\frac{\left(-H - \frac{1}{2}\right)^2 - \frac{1}{4}}{\left(1 - a(H_1 + H_2)\right)^2},\ K_{21} = 1 - \frac{\frac{1}{4} - \left(-H - \frac{1}{2}\right)^2}{\frac{2\gamma_1 k}{a}\left(1 - a(H_1 + H_2)\right)}$$

$$R_1 = \mu_1 e^{-aH_1} K_6 (K_7 - K_8 K_9 + K_8 K_{10}),\ R_2 = (-1)^H \mu_1 e^{-aH_1} K_{11} (K_{12} + K_{13} K_{14} - K_{10} K_{13}),$$

$R_3 = K_{15}(K_{16} - K_9K_{17} + K_{17}K_{18})$, $R_4 = (-1)^H K_{19}(K_{20} + K_{14}K_{21} - K_{18}K_{21})$.

Eliminating the constants A_1, B_1, D, A_2 and B_2 from eqs. (45), (46), (47), (48) and (49), we get

$$\begin{vmatrix} 0 & 0 & -K_1 & e^{iq\xi_0} & e^{-iq\xi_0} \\ 0 & 0 & -K_3 & K_2 e^{iq\xi_0} & -K_2 e^{-iq\xi_0} \\ K_4 & K_5 & 0 & -e^{iq(\xi_0 - kH_1)} & -e^{-iq(\xi_0 - kH_1)} \\ R_1 e^{-\frac{\gamma_1 k}{a} + K_9 H_1} & R_2 e^{\frac{\gamma_1 k}{a} - K_{14} H_1} & 0 & -K_2 e^{iq(\xi_0 - kH_1)} & K_2 e^{-iq(\xi_0 - kH_1)} \\ R_3 e^{-\frac{\gamma_1 k}{a} + K_9(H_1 + H_2)} & R_4 e^{\frac{\gamma_1 k}{a} - K_{14}(H_1 + H_2)} & 0 & 0 & 0 \end{vmatrix} = 0$$

$$\Rightarrow \tan(kqH_1) = Gkq \frac{\begin{matrix} K_3K_5R_3 e^{-\frac{\gamma_1 k}{a} + K_9(H_1+H_2)} - K_3K_4R_4 e^{\frac{\gamma_1 k}{a} - K_{14}(H_1+H_2)} \\ -K_1R_2R_3 e^{K_9(H_1+H_2) - K_{14}H_1} + K_1R_1R_4 e^{K_9H_1 - K_{14}(H_1+H_2)} \end{matrix}}{\begin{matrix} -K_1K_5R_3(Gkq)^2 e^{-\frac{\gamma_1 k}{a} + K_9(H_1+H_2)} + K_1K_4R_4(Gkq)^2 e^{\frac{\gamma_1 k}{a} - K_{14}(H_1+H_2)} \\ -K_3R_2R_3 e^{K_9(H_1+H_2) - K_{14}H_1} + K_3R_1R_4 e^{K_9H_1 - K_{14}(H_1+H_2)} \end{matrix}} \quad (50)$$

which is the equation governing the dispersion of torsional waves.

5.1. PROBLEM VALIDATION

When we remove the upper layer M_1, and assume the structure to be non-porous, stress-free, and homogeneous, the considered configuration simplifies to a homogeneous isotropic elastic layer on a homogeneous isotropic elastic half-space. Under these conditions, Eq. (50) takes the form as

$$\tan\left(kH_1\sqrt{\frac{c^2}{c_2^2} - 1}\right) = \frac{\mu_3}{\mu_2} \frac{\sqrt{1 - \frac{c^2}{c_3^2}}}{\sqrt{\frac{c^2}{c_2^2} - 1}}$$

which is the classical Love wave dispersion equation.

5.2. PARTICULAR CASES

Case I: Absence of inhomogeneity parameters in layer M_1, i.e. $a = b \to 0$, Eq. (50) takes the form as

$$\tan(kqH_1) = \frac{-K_3}{GkqK_1}$$

Case II: Absence of inhomogeneity parameters in half-space M_3, i.e. $m = n \to 0$, Eq. (50) takes the form as

$$\tan(kqH_1) = Gkq \frac{\begin{matrix} -\mu_3\gamma_3 kK_5R_3 e^{-\frac{\gamma_1 k}{a}+K_9(H_1+H_2)} + \mu_3\gamma_3 kK_4R_4 e^{\frac{\gamma_1 k}{a}-K_{14}(H_1+H_2)} \\ -R_2R_3 e^{K_9(H_1+H_2)-K_{14}H_1} + R_1R_4 e^{K_9H_1-K_{14}(H_1+H_2)} \end{matrix}}{\begin{matrix} -K_5R_3(Gkq)^2 e^{-\frac{\gamma_1 k}{a}+K_9(H_1+H_2)} + K_4R_4(Gkq)^2 e^{\frac{\gamma_1 k}{a}-K_{14}(H_1+H_2)} \\ +\mu_3\gamma_3 kR_2R_3 e^{K_9(H_1+H_2)-K_{14}H_1} - \mu_3\gamma_3 kR_1R_4 e^{K_9H_1-K_{14}(H_1+H_2)} \end{matrix}}$$

Case III: When the pre-stress in the layer M_2 is absent, i.e. $P \to 0$, Eq. (50) takes the form as

$$\tan\left(kH_1\sqrt{\frac{N}{G}\left(\frac{dc^2}{c_2^2}-1\right)}\right)$$

$$= Gk\sqrt{\frac{N}{G}\left(\frac{dc^2}{c_2^2}-1\right)} \frac{\begin{matrix} K_3K_5R_3 e^{-\frac{\gamma_1 k}{a}+K_9(H_1+H_2)} - K_3K_4R_4 e^{\frac{\gamma_1 k}{a}-K_{14}(H_1+H_2)} \\ -K_1R_2R_3 e^{K_9(H_1+H_2)-K_{14}H_1} + K_1R_1R_4 e^{K_9H_1-K_{14}(H_1+H_2)} \end{matrix}}{\begin{matrix} -K_1K_5R_3\left(Gk\sqrt{\frac{N}{G}\left(\frac{dc^2}{c_2^2}-1\right)}\right)^2 e^{-\frac{\gamma_1 k}{a}+K_9(H_1+H_2)} + K_1K_4R_4\left(Gk\sqrt{\frac{N}{G}\left(\frac{dc^2}{c_2^2}-1\right)}\right)^2 e^{\frac{\gamma_1 k}{a}-K_{14}(H_1+H_2)} \\ -K_3R_2R_3 e^{K_9(H_1+H_2)-K_{14}H_1} + K_3R_1R_4 e^{K_9H_1-K_{14}(H_1+H_2)} \end{matrix}}$$

Case IV: When the inhomogeneity parameters in M_1 and M_3 are absent simultaneously, i.e. $a = b \to 0, m = n \to 0$, Eq. (50) takes the form as

$$\tan(kqH_1) = \frac{\mu_3\sqrt{1-\frac{c^2}{c_3^2}}}{Gq}$$

6. NUMERICAL COMPUTATIONS AND DISCUSSIONS

Derivation of the dispersion relation reveals the relationship between phase velocity $\frac{c}{c_2}$ and wave number kH_2. The relation links phase velocity to frequency, dependent on various factors, including material properties, layer parameters and initial stress parameters $\left(\zeta = \frac{P}{2N}\right)$. The numerical values used for each medium in this analysis are as follows.

For upper heterogeneous layer M_1 [30]

$\mu_1 = 3.23 \times 10^{10}\ N/m^2, \rho_1 = 2802\ kg/m^3$

For sandwiched porous layer M_2 [30]

$G = 0.1387 \times 10^{10}\ N/m^2, N = 0.2774 \times 10^{10}\ N/m^2, \rho_{rr} = 1.926137 \times 10^3\ kg/m^3, \rho_{r\theta} = -0.002137 \times 10^3\ kg/m^3, \rho_{\theta\theta} = 0.2153337 \times 10^3\ kg/m^3$

For heterogeneous half-space M_3

$\mu_3 = 7.34\ \times 10^{10}\ N/m^2, \rho_3 = 3195\ kg/m^3$

To analyse how initial stress and material non-homogeneity in the upper layer and lower half-space impact torsional surface waves propagation, numerical calculations of phase velocity is performed using Eq. (50) for different parameter sets. MATLAB has been employed for graphical analysis and computation. In each figure, three curves are plotted, corresponding to varying one parameter at a time, while keeping the others fixed. Note that each parameter has been normalized with length. This approach allows a clear assessment of the individual contribution of each parameter to the wave propagation characteristics.

Fig. 2 explores the impact of normalized rigidity inhomogeneity parameter $\frac{a}{k}$ in upper heterogeneous layer (shown as a in the figure legend). The parameter takes values $\frac{a}{k} = 1.0, 2.0, 3.0$ with the remaining parameters fixed as $\frac{m}{k} = 1.0, \frac{n}{k} = 2.0, \frac{H_2}{H_1} = 2, f = 1, \frac{b}{k} = 1.5$. The results reveal a distinct upward shift in the dispersion curves as $\frac{a}{k}$ increases. Physically, a higher $\frac{a}{k}$ indicates a steeper exponential variation in rigidity with depth, meaning the upper layer becomes stiffer in the near-surface region. This enhanced stiffness increases the shear wave speed, thereby raising the torsional wave phase velocity. The effect is more noticeable at higher wave numbers, where shorter wavelengths interact more strongly with near-surface variations.

Fig. 3 explores the effect of normalized density inhomogeneity parameter $\frac{b}{k}$ in upper layer, with $\frac{b}{k} = 1.0, 2.0, 3.0$ and $\frac{m}{k} = 1.5, \frac{n}{k} = 2.0, \frac{H_2}{H_1} = 2, f = 1, \frac{a}{k} = 1.5$. Increasing $\frac{b}{k}$ slightly raises the phase velocity, especially for larger wavenumbers. Since higher $\frac{b}{k}$ implies a greater decrease in density with depth, the medium becomes less inertial near the surface, marginally increasing wave

speed. However, the influence is weaker compared to rigidity variation because phase velocity is more sensitive to stiffness changes than density changes in elastic wave mechanics.

Fig. 4 examines the impact of normalized rigidity inhomogeneity parameter $\frac{m}{k}$ in lower half-space, varying as $\frac{m}{k} = 1.0, 2.0, 3.0$ with $\frac{a}{k} = 1, \frac{b}{k} = 1.5, \frac{H_2}{H_1} = 2, f = 1, \frac{n}{k} = 1.5$. As marked increase in phase velocity is observed as $\frac{m}{k}$ grows. Physically, a higher $\frac{m}{k}$ signifies a stronger increase in rigidity as depth increases in lower half-space, which strengthens the substratum's ability to transmit torsional waves. This effect is significant across the entire wave number range because the lower half-space supports the wave motion over its full depth penetration.

Fig. 5 investigates the significance of normalized density inhomogeneity parameter $\frac{n}{k}$ in lower half-space for $\frac{n}{k} = 1.0, 2.0, 3.0$ with $\frac{a}{k} = 1, \frac{b}{k} = 1.5, \frac{H_2}{H_1} = 2, f = 1, \frac{m}{k} = 1.5$. The results show a consistent rise in phase velocity as $\frac{n}{k}$ increases, through the effect is moderate. A large $\frac{n}{k}$ indicates a stronger reduction of density with depth, decreasing inertia and allowing waves to penetrate more rapidly. The influence becomes more visible at higher wavenumbers, where deeper penetration causes the wave to sample more of the low-density deeper medium.

Fig. 6 presents the significance of initial stress P in porous middle layer, for $P = 1.0, 2.0, 3.0$ with $\frac{a}{k} = 1, \frac{b}{k} = 1.5, \frac{m}{k} = 1, \frac{n}{k} = 1.5, \frac{H_2}{H_1} = 2, f = 1$. The phase velocity gets significant boost by increasing compressive initial stress. This is because pre-stress effectively increases the medium's stiffness without altering its density, leading to faster shear wave propagation. The effect is prominent across all wave numbers and reflects the known phenomenon in elastic wave theory that compression raise wave speeds, while tensile pre-stress tends to reduce them.

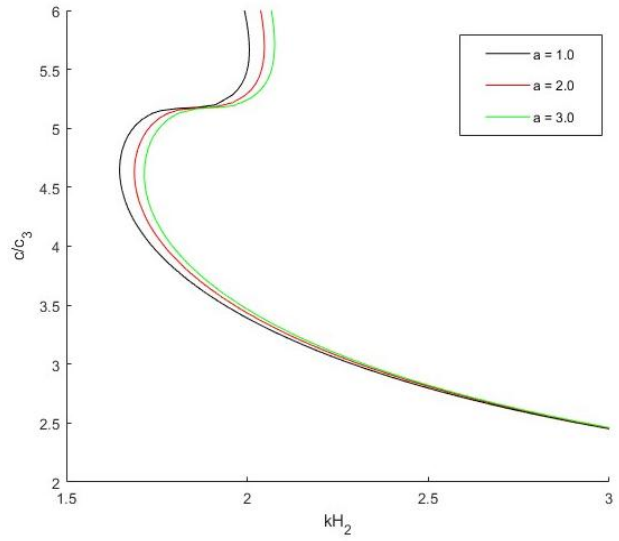


Fig. 2 Impact of $\frac{a}{k}$ on phase velocity

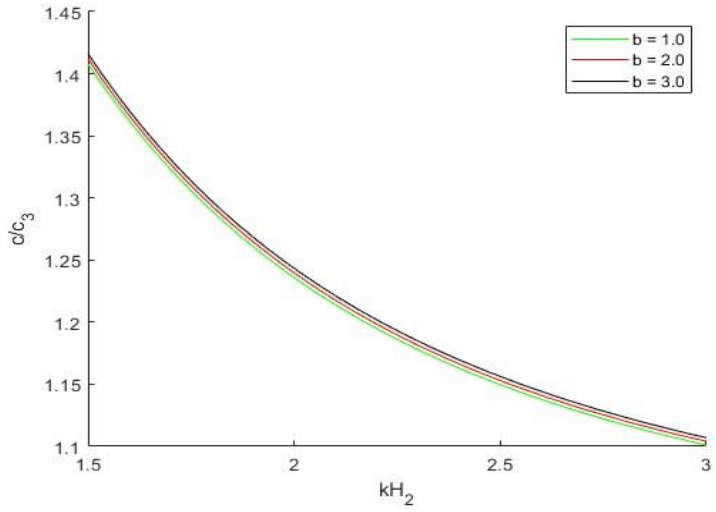


Fig. 3 Impact of $\frac{b}{k}$ on phase velocity

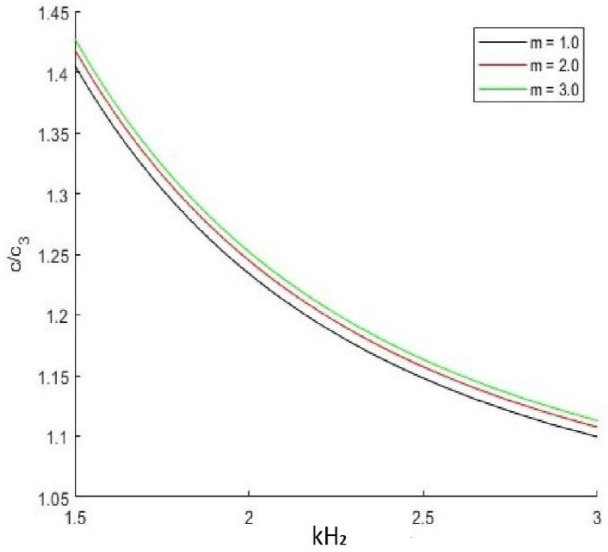


Fig. 4 Impact of $\frac{m}{k}$ on phase velocity

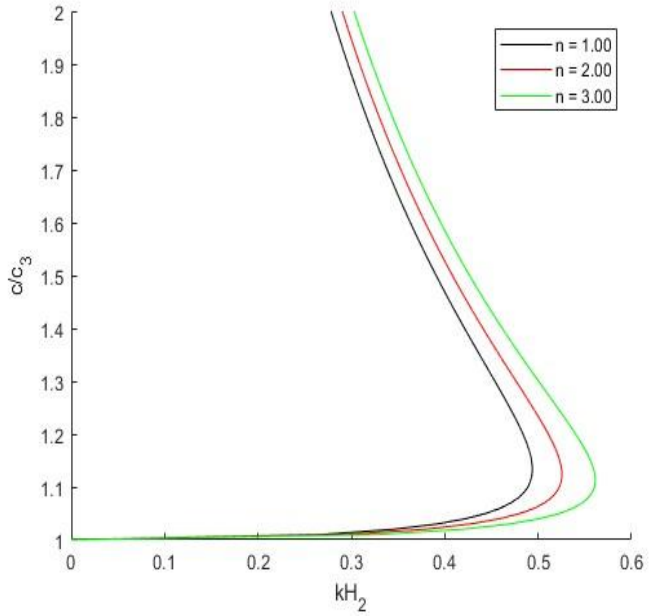


Fig. 5 Impact of $\frac{n}{k}$ on phase velocity

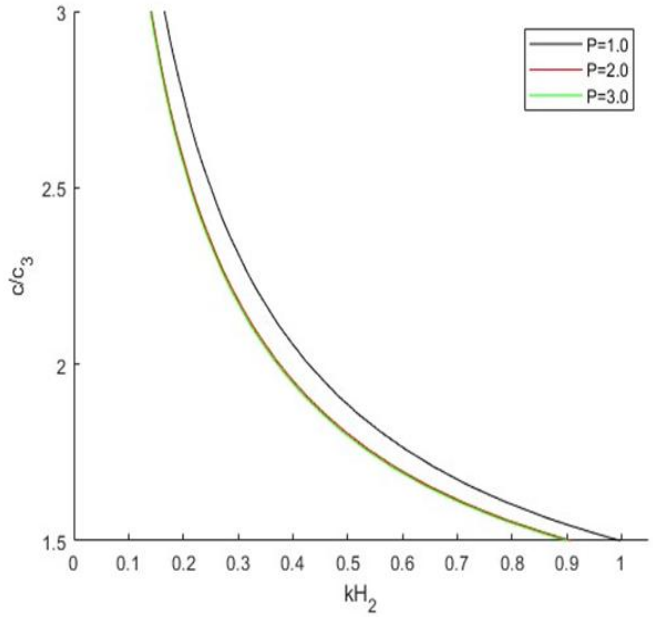


Fig. 6 Impact of P on phase velocity

7. CONCLUSION

1. Rigidity heterogeneity parameters $\frac{a}{k}$ and $\frac{m}{k}$ have the most pronounced influence, significantly increasing phase velocity of torsional surface waves.
2. Density heterogeneity parameters $\frac{b}{k}$ and $\frac{n}{k}$ cause a moderate but consistent rise in phase velocity.
3. Initial stress P in the poroelastic layer markedly enhances phase velocity by increasing the effective stiffness of the medium.
4. The effect of rigidity variation is stronger than that of density.
5. These results provide useful insights for seismic exploration, subsurface imaging, and geotechnical assessment in heterogeneous and pre-stressed geological media.

8. REFERENCES

[1] A. E. H. Love, *A Treatise on the Mathematical Theory of Elasticity*, Cambridge, U.K.: Cambridge Univ. Press, 1920.

[2] M. A. Biot, "Influence of initial stress on elastic waves," *J. Appl. Phys.*, vol. 11, no. 8, pp. 522–530, 1940, doi: 10.1063/1.1712807.

[3] W. H. Weiskopf, "Stresses in soils under a foundation," *J. Franklin Inst.*, vol. 239, no. 6, pp. 445–465, 1945, doi: 10.1016/0016-0032(45)90189-X.

[4] W. M. Ewing, W. S. Jardetzky, and F. Press, *Elastic Waves in Layered Media*, New York, NY, USA: McGraw-Hill, 1957.

[5] M. A. Biot, "Theory of propagation of elastic waves in a fluid-saturated porous solid. I. Low frequency range," *J. Acoust. Soc. Am.*, vol. 28, no. 2, pp. 168–178, 1956, doi: 10.1121/1.1908239.

[6] M. A. Biot, "Theory of propagation of elastic waves in a fluid-saturated porous solid. II. Higher frequency range," *J. Acoust. Soc. Am.*, vol. 28, no. 2, pp. 179–191, 1956, doi: 10.1121/1.1908241.

[7] M. A. Biot, *Mechanics of Incremental Deformation*, New York, NY, USA: John Wiley & Sons, 1965.

[8] M. Bath, *Mathematical Aspects of Seismology*, New York, NY, USA: Elsevier, 1968.

[9] J. D. Achenbach, *Wave Propagation in Elastic Solids*, New York, NY, USA: North-Holland, 1973.

[10] I. Vardoulakis, "Torsional surface waves in inhomogeneous elastic media," *Int. J. Numer. Anal. Methods Geomech.*, vol. 8, no. 3, pp. 287–296, 1984, doi: 10.1002/nag.1610080306.

[11] S. Dey and M. G. Sarkar, "Torsional surface waves in an initially stressed anisotropic porous medium," *J. Eng. Mech.*, vol. 128, no. 2, pp. 184–189, 2002, doi: 10.1061/(ASCE)0733-9399(2002)128:2(184).

[12] S. Dey, S. Gupta, A. K. Gupta, and S. K. Kar, "Propagation of torsional surface waves in an elastic layer with void pores over an elastic half-space with void pores," *Tamkang J. Sci. Eng.*, vol. 6, no. 4, pp. 241–249, 2003, doi: 10.6180/jase.2003.6.4.08.

[13] S. Gupta, A. Chattopadhyay, S. Kundu, *et al.*, "Effect of rigid boundary on the propagation of torsional waves in a homogeneous layer over a heterogeneous half-space," *Arch. Appl. Mech.*, vol. 80, no. 2, pp. 143–150, 2010, doi: 10.1007/s00419-009-0303-4.

[14] S. Gupta, D. K. Majhi, and S. K. Vishwakarma, "Torsional surface wave propagation in an initially stressed non-homogeneous layer over a non-homogeneous half-space," *Appl. Math. Comput.*, vol. 219, no. 6, pp. 3209–3218, 2012, doi: 10.1016/j.amc.2012.09.058.

[15] P. Kumari and V. K. Sharma, "Propagation of torsional waves in a viscoelastic layer over an inhomogeneous half space," *Acta Mech.*, vol. 225, pp. 1673–1684, 2014, doi: 10.1007/s00707-013-1021-0.

[16] P. Kumari, C. Modi, and V. K. Sharma, "Torsional waves in a magneto-viscoelastic layer over an inhomogeneous substratum," *Eur. Phys. J. Plus*, vol. 131, art. no. 263, 2016, doi: 10.1140/epjp/i2016-16263-7.

[17] S. Gupta, A. Satbhaiya, and Meena, "Effect of rigid boundary on the propagation of torsional surface waves in initially stressed gravitating dry sandy medium," *Procedia Eng.*, vol. 144, pp. 1242–1251, 2016.

[18] S. Gupta, R. Sultana, and A. K. Verma, "Existence of torsional surface wave in a porous crustal layer over an initially stressed inhomogeneous half-space," *J. Vib. Control*, vol. 22, no. 7, pp. 1717–1728, 2016, doi: 10.1177/1077546314544352.

[19] A. K. Gupta, S. Kundu, P. Patra, and A. K. Mukhopadhyay, "Effect of gravity and initial stresses on torsional surface waves in dry sandy medium under rigid layer," *Procedia Eng.*, vol. 173, pp. 1042–1047, 2017.

[20] A. Udías and E. Buforn, *Principles of Seismology*, Cambridge, U.K.: Cambridge Univ. Press, 2017, doi: 10.1017/9781316481615.

[21] S. Gupta and N. Bhengra, "Dispersion study of propagation of torsional surface wave in a layered structure," *J. Mech.*, vol. 33, no. 3, pp. 303–315, 2017.

[22] P. Alam, S. Kundu, S. Gupta, *et al.*, "Study of torsional wave in a poroelastic medium sandwiched between a layer and a half-space of heterogeneous dry sandy media," *Waves Random Complex Media*, vol. 28, no. 1, pp. 182–201, 2018, doi: 10.1080/17455030.2017.1335915.

[23] R. M. Prasad and S. Kundu, "Dispersion of torsional surface wave in a pre-stressed heterogeneous layer sandwiched between anisotropic porous half-spaces under gravity," *J. Solid Mech.*, vol. 11, no. 4, pp. 707–723, 2019, doi: 10.22034/jsm.2019.668609.

[24] S. K. Tomar and N. Kaur, "Role of sliding contact interface on torsional waves," *Math. Student*, vol. 88, pp. 125–138, 2019.

[25] P. Pati, S. Gupta, and A. Mandi, "Dispersion analysis of torsional waves in a corrugated monoclinic crystal medium cladded with a void-type porous layer and viscous-sandy substrate," *Mech. Solids*, vol. 56, no. 5, pp. 771–786, 2021, doi: 10.3103/S0025654421050010.

[26] M. Shokrollahi, M. Eskandari-Ghadi, and N. Khaji, "A unified approach for stress wave propagation in transversely isotropic elastic and poroelastic layered media," *Soil Dyn. Earthq. Eng.*, vol. 157, 107152, 2022, doi: 10.1016/j.soildyn.2022.107152.

[27] P. Kumari, S. K. Tomar, and V. K. Sharma, "Dynamical behaviour of torsional waves in a layered composite structure with sliding contact," *Arabian J. Geosci.*, vol. 15, art. no. 546, 2022, doi: 10.1007/s12517-022-09708-w.

[28] P. Kumari and Payal, "Characterization of torsional wave in a bonded corrugated dry sandy geomedia," *Mech. Solids*, vol. 58, no. 3, pp. 961–974, 2023, doi: 10.3103/S0025654423600149.

[29] S. I. Fomenko, R. B. Jana, and M. V. Golub, "Numerical modeling of elastic wave propagation in porous soils with vertically inhomogeneous fluid contents due to infiltration," *Mathematics*, vol. 11, no. 19, 4131, 2023, doi: 10.3390/math11194131.

[30] D. K. Majhi, M. Kumar, B. P. Rajak, and S. Kundu, "Effect of non-homogeneity and initial stress on torsional surface wave propagation in initially stressed poroelastic medium bounded by a heterogeneous layer and half-space," *Mech. Solids*, vol. 59, no. 2, pp. 831–845, 2024, doi: 10.1134/S0025654423602355.

Acknowledgements

The authors convey their sincere thanks to Patna University for providing facilities.

Data Availability

All data that supports the finding of this study are present in the submitted article. With the help of the data and MATLAB software, codes were generated to plot the graphs.

Conflict of Interest

The authors declared no potential conflicts of interest with respect to the research, authorship, and publication of this article.